Energy 88 (2015) 595–603

Contents lists available at ScienceDirect

Energy

journal homepage: www.elsevier.com/locate/energy

A decomposition method for network-constrained unit commitment with AC power flow constraints

Yang Bai [a], Haiwang Zhong [a,*], Qing Xia [a], Chongqing Kang [a], Le Xie [b]

[a] State Key Laboratory of Power System, Department of Electrical Engineering, Tsinghua University, Beijing 100084, People's Republic of China
[b] Department of Electrical and Computer Engineering, Texas A&M University, College Station, TX 77840, USA

ARTICLE INFO

Article history:
Received 7 March 2015
Received in revised form
26 May 2015
Accepted 29 May 2015
Available online 22 June 2015

Keywords:
Network-constrained unit commitment
AC power flow constraints
Decomposition
Power flow sensitivity

ABSTRACT

To meet the increasingly high requirement of smart grid operations, considering AC power flow constraints in the NCUC (network-constrained unit commitment) is of great significance in terms of both security and economy. This paper proposes a decomposition method to solve NCUC with AC power flow constraints. With conic approximations of the AC power flow equations, the master problem is formulated as a MISOCP (mixed integer second-order cone programming) model. The key advantage of this model is that the active power and reactive power are co-optimised, and the transmission losses are considered. With the AC optimal power flow model, the AC feasibility of the UC result of the master problem is checked in subproblems. If infeasibility is detected, feedback constraints are generated based on the sensitivity of bus voltages to a change in the unit reactive power generation. They are then introduced into the master problem in the next iteration until all AC violations are eliminated. A 6-bus system, a modified IEEE 30-bus system and the IEEE 118-bus system are used to validate the performance of the proposed method, which provides a satisfactory solution with approximately 44-fold greater computational efficiency.

1. Introduction

NCUC (Network-constrained unit commitment) is used in the smart grid operations to schedule the on/off state and power output of generators over a predefined time horizon to meet the load demand with minimizing total operating cost and satisfying various constraints [1,2]. NCUC has been widely utilized as a fundamental tool in generation scheduling [3], operations planning [4], system risk assessment [5], demand response [6] and integration of renewable energy and electric vehicles [7,8], among other functions. Prevalent NCUC models are based on the DC power flow formulation. Reactive power constraints and bus voltage limits are not considered. Hence, these NCUC models are facing challenges because the power system development yields certain new features in its operations. First, in terms of security, scarce land resources and environmental pressure enforce limits on the construction of new power plants near load centres. Currently, long-distance power transmission is crucial for supplying load demand and is expected to play an even more important role in the near future. A significant voltage drop across long-distance transmission is more likely to occur. Thus, the bus voltage limit may be violated, especially at load centre buses. In some regions, such as Spain and Texas [9], the primary concern in power grid operations is the voltage problem. Hence, it is imperative to consider bus voltage limits in NCUC. Second, to improve the economic operations, it would be beneficial to transform the perspective from dispatching the active power only to scheduling the active power and reactive power together. Because the active power and reactive power are coupled, co-optimizing them in NCUC can reduce the transmission losses, which is hard to achieve via a model that only considers the active power [10]. Based on the two reasons above, NCUC with AC power flow constraints is a necessity to improve grid operations. An effective and efficient algorithm is necessary. For ease of reference, we refer to NCUC with AC power flow constraints as *AC-NCUC* in this paper. In fact, the decoupled AC power flow model or the non-linearity effect of the AC model has begun to emerge in residual unit commitment practice in several ISOs of the U.S. [11], which exhibits the realistic significance of considering AC power flow constraints in NCUC.

Mathematically, AC-NCUC is a non-convex MINLP (mixed integer nonlinear programming) problem. While it is a challenge to

* Corresponding author. Tel.: +86 10 62794361.
E-mail address: zhonghw@tsinghua.edu.cn (H. Zhong).

http://dx.doi.org/10.1016/j.energy.2015.05.082
0360-5442/

Nomenclature

Indices

- e, i, j index for the bus in the power grid
- k index for the generation unit
- t index for the time period

Constants

- DP_k^{max}/DP_k^{min} ramping up/down power limit of unit k
- G_{ij}/B_{ij} real/imaginary elements in the ith row and jth column of the bus admittance matrix
- $NB/NG/NT$ number of buses/generation units/time periods
- $P_{i,t}^d/Q_{i,t}^d$ real/reactive load at bus i at time period t
- P_k^{max}/P_k^{min} upper/lower limit of the active power generation of unit k
- Q_k^{max}/Q_k^{min} upper/lower limit of the reactive power generation of unit k
- RS_t system spinning reserve requirement at time period t
- S_{ij}^{max} upper limit of the apparent power flow on line $i \rightarrow j$
- T_k^{on}/T_k^{off} minimum up/down time of unit k
- V_i^{max}/V_i^{min} upper/lower limit of voltage magnitude at bus i
- $y_i = g_i + \mathrm{i}\, b_i$ shunt impedance from bus i to the ground
- $z_{ij} = r_{ij} + \mathrm{i}\, x_{ij}$ complex impedance of line $i \rightarrow j$
- $\pi_{i,k}$ sensitivity of the voltage magnitude of bus i to the reactive power output of unit k

Variables

- $I_{k,t}$ unit commitment state of unit k at time period t
- $P_{k,t}/Q_{k,t}$ real/reactive power generation of unit k at time period t
- $R_{k,t}$ spinning reserve of unit k at time period t
- s_i net complex power injection at bus i
- $s_{ij} = P_{ij} + \mathrm{i}\, Q_{ij}$ complex power flow on line $i \rightarrow j$
- $S_{ij,t}$ apparent power flow on line $i \rightarrow j$ at time period t
- $SU_{k,t}/SD_{k,t}$ start-up/shut-down cost of unit k at time period t
- v_i complex voltage at bus i
- $V_{i,t}$ voltage magnitude of bus i at time period t
- $X_{k,t}^{on}/X_{k,t}^{off}$ on/off time of unit k at time period t
- $\theta_{ij,t}$ voltage phase difference between bus i and bus j at time period t

solve non-convex MINLP problems with state-of-the-art techniques in a robust and efficient way [12], considerable effort is still devoted to exploiting various decomposition methods to solve AC-NCUC. Using the LR method and a variable duplication technique, AC-NCUC is decomposed into a series of single-unit UC problems and single-period OPF (optimal power flow) problems in Ref. [13]. As noted in Ref. [13], its OPF-intensive feature may cast doubt on its efficiency. BD (benders decomposition) is used to decompose AC-NCUC into a DC power flow-based UC master problem and OPF-based subproblems for the security check in Ref. [14]. Several strategies are studied in Ref. [15] to accelerate the computation. For this *non-convex* MINLP AC-NCUC problem, it is worth clarifying that an ideal algorithm that finds a global optimum with a flawless convergence guarantee is not yet resolved. This paper does not intend to offer this type of algorithm but make progress by providing a decomposition method with improved modelling, satisfactory solutions and high efficiency. As the literature review suggests, although the master-slave decomposition strategy is a natural choice for solving AC-NCUC, different models in both master and slave levels and diverse feedback constraints would likely lead to different performances. More effort should be made to improve the master problem modelling and feedback constraints, which is exactly what this paper intends to contribute.

Compared with the DC power flow-based NCUC model, which is a MILP (mixed integer linear programming) problem, the AC-NCUC model is significantly more complicated due to the non-convexity and nonlinearity of the AC power flow equations. Recently, with the development of SDP (semi-definite programming) and SOCP (second-order cone programming), one possibility is to remodel AC power flow equations, transforming the ACOPF model from a non-convex NLP problem into an SDP or SOCP problem under some assumptions. This approach includes two typical formulations. One formulation focuses on the bus injection model in the rectangular coordinate form and formulates ACOPF as an SDP problem [16,17]. By relaxing the integer constraints, the SDP model is used as a basis to solve AC-NCUC in Ref. [18]. To obtain an integer solution, a heuristic rounding process is necessary. However, feasibility is not guaranteed in this process. The other formulation studies the branch flow model, which relaxes the bus angle to formulate ACOPF into an SOCP model [19–21]. This formulation has been applied in transmission planning [22]. In addition, SOCP is used to solve unit commitment problem without considering network constraints in Ref. [23]. The two formulations provide new ways and make important progress in solving OPF problems. However, for meshed networks, neither of them is a "perfect" equivalent to the original AC power flow equations. To be a "perfect" equivalent, a rank condition is necessary in Refs. [16], and phase shifters should be applied as claimed in Ref. [20].

Despite this "imperfect equivalence", the power flow formulations in the SDP and SOCP models can be considered as convex *approximations* of the original AC power flow equations. It would be beneficial to properly utilize these convex approximations when solving various problems, such as ACOPF, UC, and power system planning. This is because the approximations contain most of the active-reactive power coupling physics in the original AC model, which can be used as basis of solving non-convex problems. The motivation for doing so lies in the possible improvement of the overall computational efficiency because solving the convex approximation model is usually easier than solving the original non-convex model.

With this basic idea, a decomposition method to solve the AC-NCUC problem is proposed in this paper. Highlights of the proposed method are summarized as follows.

First, the branch flow model is used to formulate a MISOCP (mixed integer second-order cone programming) model as the master problem. Compared with the DC power flow-based master problem model that only considers the active power, the MISOCP model considers both the active power and reactive power balance as well as the transmission losses. Thus, it respects part of the nonlinear physics in the AC power flow equations instead of considering only simplified linear relations. This is effective in committing not only the generating units for the active load but also those units necessary to supply the reactive load, which are often ignored in DC power flow-based models. As a result, the UC result of the proposed master problem can satisfy most AC power flow constraints in the original MINLP model, which helps decrease the AC violations in the subproblems and eventually aids in reducing iterations and enhances the overall computational efficiency.

Second, based on the UC result of the master problem, an AC power flow feasibility check is conducted for each time period in the subproblems. The OPF-based models in the subproblems enable a precise consideration of the bus voltage and transmission flow constraints. By properly setting the slack variables, bus voltage violations caused by inappropriate UC results are identified. To further improve the computational efficiency, the parallel computing techniques are used.

Third, to eliminate bus voltage violations, feedback constraints are generated based on the relationship between the bus voltage and the unit reactive power generation. These constraints contain the information on which units are most effective in eliminating voltage violations and the quantitative effect of these units' reactive power generation on the bus voltage magnitude. By introducing them into the master problem, the UC result can be adjusted accordingly to correct the bus voltage violations iteratively. Although they are linear similar to Benders cuts, these constraints have a clear physical interpretation, and they are more effective because each constraint corresponds to a specific bus voltage violation. They are not dependent on the master problem formulation and may be used wherever "AC power flow feasibility repairing" is necessary.

The remainder of the paper is organized as follows. Section 2 presents the MINLP formulation of the AC-NCUC problem. Section 3 provides the proposed decomposition method for AC-NCUC. Section 4 covers case studies on three systems. Section 5 concludes the paper.

2. AC-NCUC problem formulation

Mathematically, AC-NCUC is a *non-convex* MINLP problem. Its typical objective is to minimize the sum of the production cost, startup cost and shutdown cost of generating units as:

$$min\sum_{k=1}^{NG}\sum_{t=1}^{NT}\left[F_k(P_{k,t})+SU_{k,t}+SD_{k,t}\right]. \tag{1}$$

where $F_k(\cdot)$ is the quadratic production cost function of unit k. The constraints include the AC power flow equations (2) and (3), system spinning reserve requirements (4), unit ramping limits (5) and (6), unit minimum on/off time limits (7) and (8), unit active power and reactive power generation limits (9) and (10), transmission flow limits (11) and bus voltage magnitude limits (12).

$$\sum_{k\in i}P_{k,t}-V_{i,t}\sum_{j\in i}V_{j,t}\left(G_{ij}\cos\theta_{ij,t}+B_{ij}\sin\theta_{ij,t}\right)=P_{i,t}^{d}\quad\forall i,\forall t \tag{2}$$

$$\sum_{k\in i}Q_{k,t}-V_{i,t}\sum_{j\in i}V_{j,t}\left(G_{ij}\sin\theta_{ij,t}-B_{ij}\cos\theta_{ij,t}\right)=Q_{i,t}^{d}\quad\forall i,\forall t \tag{3}$$

$$\sum_{k=1}^{NG}R_{k,t}\geq RS_t\quad\forall t \tag{4}$$

$$P_{k,t}-P_{k,(t-1)}\leq DP_k^{\max}I_{k,(t-1)}+\left[I_{k,t}-I_{k,(t-1)}\right]P_k^{\min}+P_k^{\max}\left(1-I_{k,t}\right)\quad\forall t,\forall k \tag{5}$$

$$P_{k,(t-1)}-P_{k,t}\leq DP_k^{\min}I_{k,t}-\left[I_{k,t}-I_{k,(t-1)}\right]P_k^{\min}+P_k^{\max}\left[1-I_{k,(t-1)}\right]\quad\forall t,\forall k \tag{6}$$

$$\left[X_{k,(t-1)}^{on}-T_k^{on}\right]*\left[I_{k,(t-1)}-I_{k,t}\right]\geq 0\quad\forall t,\forall k \tag{7}$$

$$\left[X_{k,(t-1)}^{off}-T_k^{off}\right]*\left[I_{k,t}-I_{k,(t-1)}\right]\geq 0\quad\forall t,\forall k \tag{8}$$

$$I_{k,t}P_k^{\min}\leq P_{k,t}\leq I_{k,t}P_k^{\max}\quad\forall t,\forall k \tag{9}$$

$$I_{k,t}Q_k^{\min}\leq Q_{k,t}\leq I_{k,t}Q_k^{\max}\quad\forall t,\forall k \tag{10}$$

$$S_{ij,t}\leq S_{ij}^{\max}\quad\forall t,\forall(i\to j) \tag{11}$$

$$V_i^{\min}\leq V_{i,t}\leq V_i^{\max}\quad\forall i,\forall t \tag{12}$$

where $k\in i$ denotes that unit k is located at bus i and $j\in i$ denotes that bus j is connected with bus i. Because this paper focuses on solving AC-NCUC with the proposed decomposition method, the non-unity transformer tap, non-zero phase shifter and shunt charging capacitances are assumed to be constant in this paper for simplicity, and the impact of optimizing them will be studied in future work. Please refer to [24] for detailed formulations of $R_{k,t}, X_{k,t}^{on}, X_{k,t}^{off}, SU_{k,t}, SD_{k,t}$ and [25] for $S_{ij,t}$.

3. The proposed decomposition method

3.1. The decomposition strategy of the proposed method

It is a highly intractable computational task to directly solve the AC-NCUC model as formulated in Section 2 for large-scale systems. Instead, a decomposition method is proposed in this paper. Its structure is shown in Fig. 1. At the upper level, the master problem is formulated as an MISOCP problem with conic approximations of AC power flow equations and with consideration for all of the operational constraints and binary variables. At the lower level, based on the ACOPF model, the subproblems are formulated for each time period to determine whether the AC power flow is feasible given the master problem's UC result. When the AC power flow is infeasible for certain time periods, feedback constraints are formulated and introduced to the master problem as additional

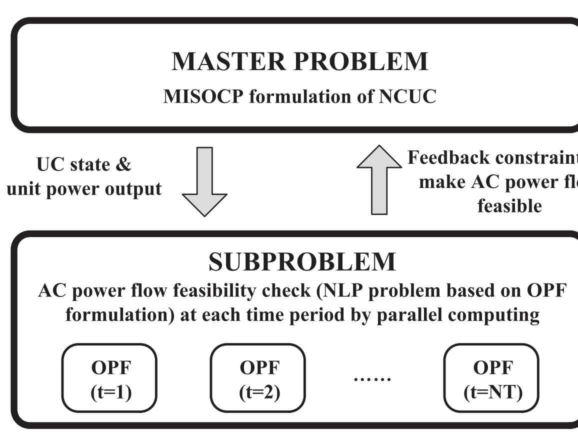

Fig. 1. The structure of the proposed method.

constraints for the next iteration. The iteration terminates when AC power flow is feasible at each time period.

3.2. The master problem

According to the aforementioned decomposition strategy, quadratic constraints are formulated based on the branch flow model to approximate the AC power flow equations (2) and (3). With these quadratic constraints replacing (2) and (3) to model the power flow, an MISOCP model is formulated. Denote line l as $l(i,j)$ or $(i \rightarrow j)$ if it points from bus i to bus j. The subscript t is dropped for notation simplicity in (13) through (20).

In accordance with the power balance at each bus,

$$\sum_{e:j\rightarrow e} s_{je} - \sum_{i:i\rightarrow j}\left(s_{ij} - z_{ij}|s_{ij}|^2 \Big/ V_i^2\right) + y_j^* V_j^2 = s_j \quad \forall j, \tag{13}$$

and based on Ohm' law,

$$v_j = v_i - z_{ij}s_{ij}^* \Big/ v_i^* \quad \forall l(i,j), \tag{14}$$

where s_{ij}^*/v_i^* is the conjugate current on line $l(i,j)$. Hence, $|s_{ij}|^2/V_i^2$ is the magnitude square of the current on line $l(i,j)$. Take the magnitude squared of (14). Then,

$$V_j^2 = V_i^2 + |z_{ij}|^2|s_{ij}|^2 \Big/ V_i^2 - \left(z_{ij}s_{ij}^* + z_{ij}^*s_{ij}\right) \quad \forall l(i,j). \tag{15}$$

Using real variables, (13) and (15) are formulated as follows:

$$\sum_{k\in j} P_k - P_j^d = \sum_{e:j\rightarrow e} P_{je} - \sum_{i:i\rightarrow j}(P_{ij} - r_{ij}h_{ij}) + g_j V_j^2 \quad \forall j \tag{16}$$

$$\sum_{k\in j} Q_k - Q_j^d = \sum_{e:j\rightarrow e} Q_{je} - \sum_{i:i\rightarrow j}(Q_{ij} - x_{ij}h_{ij}) + b_j V_j^2 \quad \forall j \tag{17}$$

$$V_j^2 = V_i^2 - 2(r_{ij}P_{ij} + x_{ij}Q_{ij}) + \left(r_{ij}^2 + x_{ij}^2\right)h_{ij} \quad \forall l(i,j) \tag{18}$$

$$h_{ij}V_i^2 = P_{ij}^2 + Q_{ij}^2 \quad \forall l(i,j) \tag{19}$$

Equations (16) through (19) are referred to as the relaxed branch flow model in Ref. [19]. By relaxing the "=" in (19) to "≥", we have

$$h_{ij}V_i^2 \geq \left(P_{ij}^2 + Q_{ij}^2\right) \quad \forall l(i,j). \tag{20}$$

By replacing (2) and (3) with (16) through (18) and (20), the MINLP model in Section 2 is transformed into an MISOCP model, where V_i^2 is a variable. This model transformation yields two consequences.

First, because the objective of the model is to minimize the total cost of the active power generation, the transmission loss tends to be reduced by optimization. Because $r_{ij}h_{ij}$ represents the transmission loss across line $l(i,j)$, optimization tends to reduce h_{ij}. Although it is not guaranteed analytically, the "≥" in (20) tends to be equal ("="). In some cases, the "≥" in (20) might end with ">" in the optimal solution. Thus, the transmission loss may be overestimated.

Second, it is noted that the magnitude is squared to derive (15) from (14). Thus, (15) and (18), which is derived from (15), lose the angle equality information implied in (14), and only the magnitude equality is retained.

Due to these two consequences, (16) through (18) and (20) are not always equivalent to (2) and (3). Thus, the MISOCP model solution is not always equivalent to the MINLP model solution. We refer readers to [19], which comments that the "≥" in (20) always ends with an exact ("=") equation under several nontrivial assumptions and proposes the *angle recovery condition* under which the angle equality implied in (14) holds in the solution based on (16) through (18) and (20). Unfortunately, for the AC-NCUC problem considered in this paper, those assumptions are not appropriate, and the *angle recovery condition* does not always hold. Hence, the MISOCP model is not equivalent to the original MINLP model. However, the MISOCP model satisfies the power balance at each bus, considers the complex power losses and only relaxes the voltage angle.

It is worth emphasizing that V_i^2 is taken as a variable thus far. To further simplify the model, we attempt to take it as a constant in the master problem and update it at each iteration. The motivation is that by relaxing V_i^2, (18) is eliminated, and V_i^2 in (16), (17) and (20) is constant, which may help ease the computational burden because there are fewer variables and a simpler constraint formulation. The precise calculation of V_i^2 is achieved via the subproblems. However, it is still possible for us to take V_i^2 as a variable in the master problem model when it is necessary (see Section 3.4).

Therefore, the MISOCP master problem model in this paper consists of (1) as the objective function and (4) through (12), (16), (17) and (20) as the constraints. Note that the only non-convexity in the MISOCP model is in the integer constraints. It is difficult to analytically quantify the error between the MISOCP and original MINLP models, which might be the subject of future work. However, numerical tests in Ref. [22] offer evidence that the solution based on (16), (17) and (20) provides a closer objective value to the true objective than the DC approximation, even though it may not be generally true in every circumstance.

It is worth emphasizing that the main motivation for using the MISOCP model as the master problem is to obtain a UC state result as close to the UC state result of the MINLP model as possible with a high computational efficiency. In certain cases, the numerical results are promising. However, it is possible that the AC power flow at a certain time period is infeasible given the UC result of the MISOCP model. Note that "*infeasible*" indicates that an AC power flow solution satisfying bus voltage and transmission flow limits does not exist. Identifying the infeasible periods, measuring the infeasibility and introducing feedback constraints to the master problem to correct this infeasibility are exactly the tasks that should be performed via the subproblems.

3.3. The subproblems

To this end, according to the UC result of the master problem, the subproblem of each time period is formulated based on the ACOPF model. It is an NLP problem formulated as follows. In (21) through (26), the subscript t indicating the particular time period is omitted for notation simplicity.

$$\min \sum_{i=1}^{NB}(d_{i,1} + d_{i,2}), \tag{21}$$

s.t.
Power flow Equations (2) and (3)

$$P_k - \widehat{P}_k = 0 \quad \forall k \tag{22}$$

$$\widehat{I}_k Q_k^{\min} \leq Q_k \leq \widehat{I}_k Q_k^{\max} \quad \forall k \tag{23}$$

$$S_{ij} \leq S_{ij}^{\max} \quad \forall l(i,j) \tag{24}$$

$$V_i^{\min} \le V_i + d_{i,1} - d_{i,2} \le V_i^{\max} \quad \forall i \tag{25}$$

$$d_{i,1} \ge 0, d_{i,2} \ge 0 \quad \forall i. \tag{26}$$

where $\widehat{I}_k, \widehat{P}_k$ denote the corresponding UC state and active power generation of the master problem solution, respectively. The objective function of this model is to minimize the total violation of the bus voltage magnitude limits. With the accurate AC power flow equations (2) and (3), constraints (22) through (25) represent the limits on the active power generation, limits on the reactive power generation, limits on the transmission line flow and limits on the bus voltage magnitudes, respectively. Three key features of these constraints are as follows.

First, slack variables $d_{i,1}, d_{i,2}$ are only introduced into the bus voltage magnitude constraints (25). This indicates that only bus voltage magnitude constraints can be violated and that other constraints should be strictly satisfied. Hence, if all slack variables are zero, a feasible AC power flow is found. If certain slack variables are nonzero, their values are considered as a metric of the AC infeasibility and used to formulate feedback constraints to eliminate this infeasibility.

Second, as shown in (22), the unit active power generation variables are fixed to the corresponding $P_{k,t}$ value of the master problem solution to avoid violating ramping constraints (5) and (6), which have been satisfied in the master problem solution [14]. Because the AC power flow infeasibility is mostly due to the voltage violation arising from redundant or insufficient reactive power injection, fixing the unit active power output will not significantly worsen the infeasibility.

Third, because the unit reactive power generation is typically regarded as time-decoupled in NCUC study, it is optimised in our subproblems, as shown in (23). Note that reactive power generations are limited to zero for OFF units in the master problem solution. An insight highlighted herein is that with the objective of minimizing the sum of slack variables in the bus voltage magnitude constraints, the optimization of unit reactive power generations is actually the process of determining whether a feasible AC power flow solution exists based on the UC state of the master problem solution.

In addition, because these *NT* subproblems of different time periods are decoupled, the parallel computing technique is employed to accelerate the computation.

3.4. Feedback constraints between the master problem and subproblems

If the objective values of the *NT* subproblems are all zero, which indicates that all of the $d_{i,1}, d_{i,2}$ are zeros and that a feasible AC power flow solution exists at every period, the algorithm ends. If $d_{i,1} > 0$ or $d_{i,2} > 0$ at a certain time period, which indicates a voltage violation at bus *i*, it can be concluded that a feasible AC power flow solution cannot be obtained at this time period based on the UC state of the master problem solution. The UC state needs to be adjusted to eliminate the voltage violation.

In normal operating conditions, according to the MW-θ/Mvar-V decoupling principle, the bus voltage magnitude is mainly influenced by the reactive power injection [29]. Using this knowledge, the feedback constraints that compensate for the bus voltage violation through a change in the unit reactive power generation are formulated based on the sensitivity $\pi_{i,k}$ of the bus voltage magnitude to a change in the unit reactive power generation (see the Appendix for the derivation). These feedback constraints are denoted as *V-Q constraints* for brevity.

When $d_{i,1} > 0$, which indicates that the voltage at bus *i* needs to be higher, the V-Q constraint is

$$\sum_{k=1}^{NG} \pi_{i,k}\left(Q_k - \widehat{Q}_k\right) - \widehat{d}_{i,1} \ge 0. \tag{27}$$

When $d_{i,2} > 0$, which indicates that the voltage at bus *i* needs to be lower, the V-Q constraint is

$$\sum_{k=1}^{NG} \pi_{i,k}\left(Q_k - \widehat{Q}_k\right) + \widehat{d}_{i,2} \le 0, \tag{28}$$

where $\widehat{d}_{i,1}, \widehat{d}_{i,2}$ are the $d_{i,1}, d_{i,2}$ values of the subproblem solutions, respectively, and $\widehat{Q}_k$ is the Q_k value of the master problem solution from the previous iteration. Hence, the previous master problem solution always violates the new V-Q constraints (27) or (28). These constraints are valid for the iteration to proceed. Discussions on (27) and (28) follow.

First, although (27) and (28) do not directly constrain the UC state variable $I_{k,t}$, they can influence the value of $I_{k,t}$ via $Q_{k,t}$ because $I_{k,t}$ and $Q_{k,t}$ are coupled in (10). For example, if unit *k* is OFF in the previous iteration and it must supply the reactive power to satisfy (27) or (28) at time period *t*, $Q_{k,t}$ changes from zero to nonzero. With the effect of (10), $I_{k,t}$ changes from zero to one consequently. It is also worth noting that all units, whether ON or OFF in the master problem solution from the previous iteration, are included in (27) and (28).

Second, each voltage violation corresponds to a specific V-Q constraint associated with the violation amount and related units. Compared with other types of feedback constraints, *e.g.*, the traditional Benders cut which combines the violation information in one single constraint, each V-Q constraint is more focused on the voltage violation that it is "responsible" for correcting. Hence, the V-Q constraint is expected to be more effective. Consequently, the number of V-Q constraints equals to the number of bus voltage violations.

Third, the sensitivity $\pi_{i,k}$ in the V-Q constraints is derived from the extension of the B'' matrix used in the fast decoupled power flow method. As a result, $\pi_{i,k}$ is constant for a given power grid and does not require recalculation in successive iterations. Thus, formulating (27) and (28) hardly affects the overall computational efficiency of the proposed algorithm.

In addition to introducing (27) and (28) into the master problem, the bus voltage magnitudes $V_{i,t}$ in the master problem at each iteration are updated to the corresponding values in the subproblem solutions of the previous iteration. The initial value of the first iteration is set to 1.0 p.u. The updated voltages improve the approximation accuracy of the MISOCP model, which aids in reducing iterations effectively. In most cases, V-Q constraints and this V updating strategy work well without convergence difficulty. However, in case that some heavily loaded systems need to adjust active power injections to solve voltage problems, when voltage violations cannot be corrected with the V-Q constraints after a significant number of iterations, we make an automatic switch to recover V_i^2 as variables in the master problem (still an MISOCP model) to enable the co-optimization of the active power and bus voltage.

4. Case studies

A 6-bus system, a modified IEEE 30-bus system and the IEEE 118-bus system are used to analyse the performance of the proposed method. The 6-bus system case mainly compares the performances of the proposed master problem model and the traditional DC power flow-based UC model to illustrate the advantage of the former. The modified IEEE 30-bus system case presents the iterative process in detail to verify the principle of the proposed method. The IEEE 118-bus system case focuses on validating the computational efficiency, accuracy and robustness of the proposed method. In all case studies, the AC-NCUC with a time horizon of 24 time periods (24 h) is considered. A computer with a 2.4 GHz Intel Core i5 CPU is used to perform the computations. The MISOCP models are solved using Gurobi 5.6.2 [26], and the NLP models are solved using Ipopt [27]. Three parallel computing cores are used to solve the subproblems.

4.1. A 6-bus system

The 6-bus system data can be found in Ref. [14]. A single line diagram of the system is depicted in Fig. 2. It has three generators, five transmission lines and two transformers. The ratios of active loads and reactive loads at buses 3, 4 and 5 are assumed as $P^d_{3,t} : P^d_{4,t} : P^d_{5,t} = 1{:}\ 1.57{:}\ 2.05$ and $Q^d_{3,t} : Q^d_{4,t} : Q^d_{5,t} = 1 : 1.21 : 2.41$, respectively. Three scenarios are tested.

Scenario 0: Solve the MINLP model formulated in Section 2 using the MINLP solver GAMS/SBB [28]. This scenario serves as the benchmark.

Scenario 1: Solve the MISOCP model formulated in the master problem. Then, based on the UC result, determine the AC power flow feasibility for each hour (*i.e.*, for each hour, solve the subproblems proposed in Section 3.3 to check whether there is violated bus voltage).

Scenario 2: Solve the DC power flow-based UC model [14], which is an MILP problem. Then, based on the UC result, determine the AC power flow feasibility for each hour.

The UC state result of Scenario 0 is shown in Table 1. After an exhaustive search for this small system, we find that it is the global optimum. The UC state of Scenario 1 is identical to that of Scenario 0. Therefore, when we determine the AC power flow feasibility for each hour based on the UC result of Scenario 1, the AC power flow is feasible at each hour, as expected. The UC state result of Scenario 2 is shown in Table 2. When we determine the AC feasibility for each hour based on this UC result, the bus voltage is violated at hours 1 through 9 and 24 due to the following:

1) G3 is not committed at hours 1 through 9 and 24. Thus, only G1 supplies the loads during these hours. G1 can supply all active power loads. However, for hours 1, 8, 9 and 24, the total reactive load (50.37, 51.06, 53.71 and 56.23 Mvar, respectively) exceeds the $Q_k^{\max}$ of G1 (50 Mvar), which indicates that G1 alone cannot supply all of the reactive loads during these hours.
2) For hours 2 through 7, the $Q_k^{\max}$ of G1 is larger than the total reactive load. However, the reactive load at bus 5, which is relatively far from G1, is heavy. Only committing G1 among all three generators is not adequate to supply all reactive loads with the reactive transmission loss.

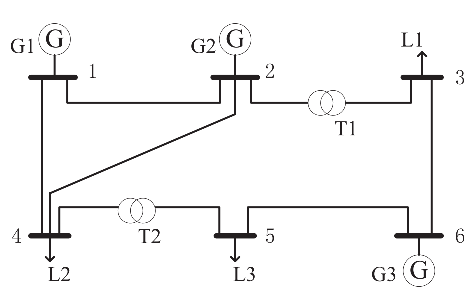

Fig. 2. The single line diagram of the 6-bus system.

Table 1
UC state of scenarios 0 & 1 in the 6-bus system.

Units	Hours (1–24)					
	1–4	5–8	9–12	13–16	17–20	21–24
G1	1 1 1 1	1 1 1 1	1 1 1 1	1 1 1 1	1 1 1 1	1 1 1 1
G2	0 0 0 0	0 0 0 0	0 1 1 1	1 1 1 1	1 1 1 1	1 1 0 0
G3	1 1 1 1	1 1 1 1	1 1 1 1	1 1 1 1	1 1 1 1	1 1 1 1

Table 2
UC state of scenario 2 in the 6-bus system.

Units	Hours (1–24)					
	1–4	5–8	9–12	13–16	17–20	21–24
G1	1 1 1 1	1 1 1 1	1 1 1 1	1 1 1 1	1 1 1 1	1 1 1 1
G2	0 0 0 0	0 0 0 0	0 1 1 1	1 1 1 1	1 1 1 1	1 1 0 0
G3	0 0 0 0	0 0 0 0	0 1 1 1	1 1 1 1	1 1 1 1	1 1 1 0

In Scenario 2, the MILP UC model, which is based on the DC power flow, only considers the active load balance without modelling the reactive power. Consequently, its UC result may not satisfy the reactive load balance, even though the active load balance is satisfied. By contrast, the MISOCP master problem in this paper formulates both the active power and reactive power, which aids in committing the necessary units for both active load balance and reactive load balance, especially those necessary for reactive power supply and voltage support (G3 in this case). These units may not be committed in DC power flow-based UC models. Therefore, compared with the MILP type of master problem (*e.g.*, the formulation used in Ref. [14]), the UC state result of the MISOCP master problem is probably closer to that of the original MINLP problem as formulated in Section 2. As an example, in this 6-bus system case, the proposed method needs only one iteration to converge to the optima, while the method using a MILP master problem requires more iterations to obtain the same result. Thus, it would be beneficial to use the MISOCP model in the master problem for fewer voltage violations in subproblems, which yields fewer iterations and higher efficiency for the overall computation. This benefit would be large especially for the cases where the reactive power and voltage have a significant impact on the UC schedule, *i.e.*, the cases where the DC power flow-based UC is probably AC infeasible and the AC-NCUC is imperative.

4.2. A modified IEEE 30-bus system

A modified IEEE 30-bus system [30], depicted in Fig. 3, is used to illustrate the iteration process of the proposed method. The generator data, unit cost coefficients and hourly loads are shown in Tables 3–5, respectively. Due to the lack of shutdown cost data, the

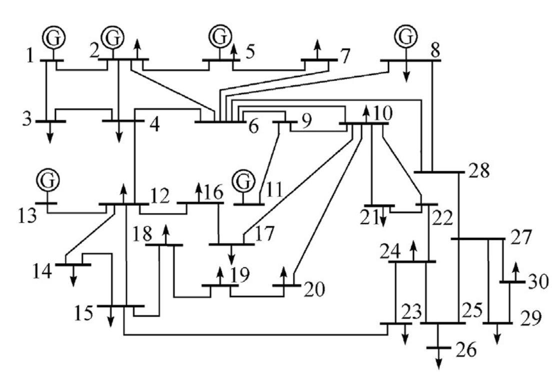

Fig. 3. The single line diagram of the IEEE 30-bus system.

Table 3
Modified generator data for the IEEE 30-bus system.

	Pmax/Pmin (MW)	Qmax/Qmin (Mvar)	Min up/down (h)	Ramp (MW/h)
G1	200/40	60/−20	8/8	60
G2	80/20	60/−20	4/4	30
G3	50/10	63/−15	4/4	30
G4	35/0	50/−15	2/2	30
G5	30/5	40/−10	2/2	30
G6	40/15	45/−15	4/4	30

Table 4
Generator quadratic production costs and start-up costs.

	a(MBtu/MW^{2}h)	b(MBtu/MWh)	c(MBtu)	Start-up (MBtu)
G1	0.1	16	120	400
G2	0.1	21	140	160
G3	0.1	22	140	100
G4	0.1	23	145	70
G5	0.1	23	145	60
G6	0.1	25	155	80

Table 5
Hourly load for the IEEE 30-bus system.

Hour	Pd (MW)	Qd (Mvar)	Hour	Pd (MW)	Qd (Mvar)
1	193.94	86.36	13	268.10	119.39
2	182.83	81.41	14	269.67	120.09
3	175.65	78.22	15	275.50	122.68
4	171.29	76.28	16	283.17	126.10
5	171.66	76.44	17	283.40	126.20
6	177.66	79.11	18	273.15	121.64
7	191.95	85.48	19	272.30	121.26
8	196.61	87.55	20	262.75	117.01
9	206.81	92.09	21	262.71	116.99
10	229.11	102.03	22	257.57	114.70
11	253.08	112.70	23	216.90	96.59
12	261.37	116.39	24	216.54	96.43

shutdown cost of each generator is assumed to be zero in this case, which will not essentially reduce the complexity of the problem or affect the performance of the proposed method.

Two iterations are required for the proposed method to solve the AC-NCUC model. After the first iteration, as shown in Table 6, the economical units G1 and G4 are used as base units, and the expensive unit G6 is not committed. The remaining units are committed accordingly to satisfy the hourly load. Next, based on the UC state in Table 6, the subproblems proposed in Section 3.3 are solved for each hour. The result indicates 16 voltage violations at buses 18, 19, 23, 24 and 26. All of the violations occur at hours 1, 2, 7 and 8, and all of them violate the lower limit (0.95 p.u.). The maximum violation of 0.0027 p.u. occurs at bus 26 at hour 8.

Generally, the bus voltage violates the lower limit when the reactive power supply is insufficient, which indicates that more units should be committed to increase the reactive power injection. The sensitivity $\pi_{i,k}$ of the voltage magnitude at the violated buses to

Table 6
UC state after iteration 1 in the IEEE-30 case.

Units	Hours (1–24)					
	1–4	5–8	9–12	13–16	17–20	21–24
G1	1 1 1 1	1 1 1 1	1 1 1 1	1 1 1 1	1 1 1 1	1 1 1 1
G2	0 0 0 0	0 0 0 0	0 0 0 0	0 1 1 1	1 0 0 0	0 0 0 0
G3	0 0 0 0	0 0 0 0	1 1 1 1	1 1 1 1	1 1 1 1	1 1 1 1
G4	1 1 1 1	1 1 1 1	1 1 1 1	1 1 1 1	1 1 1 1	1 1 1 1
G5	0 0 0 0	0 0 0 0	0 0 1 1	1 1 1 1	1 1 1 1	1 1 0 0
G6	0 0 0 0	0 0 0 0	0 0 0 0	0 0 0 0	0 0 0 0	0 0 0 0

Table 7
V-Q sensitivity between the voltage-violated buses and generators.

	G1	G2	G3	G4	G5	G6
B18	0.0453	0.0775	0.1039	0.1798	0.1953	0.2152
B19	0.0455	0.0773	0.1047	0.1847	0.1877	0.2044
B23	0.0458	0.0771	0.1060	0.1729	0.1772	0.1926
B24	0.0457	0.0751	0.1073	0.1483	0.1468	0.1568
B26	0.0456	0.0739	0.1081	0.1333	0.1283	0.1350

a change in reactive power generation of the six generators is calculated according to the Appendix and is shown in Table 7. Accordingly, 16 V-Q constraints are introduced to the master problem for the second iteration. Next, the updated master problem is solved, and based on the new UC state result as shown in Table 8, the subproblems are solved again. The result indicates no voltage violation at any hour, which means that the AC-NCUC is successfully solved and the algorithm ends. Comparing the result in Table 6 with Table 8, we note that with the effect of the V-Q constraints introduced in the second iteration, G5 is newly committed at hours 1 and 2, and G3 is newly committed at hours 7 and 8. With the additional reactive power supplied by G3 and G5, the voltages that were violated in the first iteration recovered to approximately 0.97 p.u., which is within their limits.

4.3. The IEEE 118-bus system

Consisting of 54 units and 186 transmission lines, the IEEE 118-bus system [30] is used to validate the scalability of the proposed method. The 24-h system load profile is based on the typical load profile of a realistic power system in China with a minimum load (2820 MW/1079 Mvar) at time period 4 and a maximum load (4666 MW/1735 Mvar) at time period 17.

Two iterations are used by the proposed method to solve the AC-NCUC in this case. After the first iteration, 183 voltage violations occur at hours 1 through 6, 11, and 14 through 22. The voltage violated buses are mainly located in the areas around buses 77 through 92 and 104 through 112. Accordingly, 183 V-Q constraints are introduced to the master problem. With their effect, Unit 45 is newly committed at hours 1 through 6, and Unit 52 is newly committed at hours 11 through 22. Based on this updated UC state, no voltage violations occur at any hour.

The MINLP model in Section 2 is formulated for this case and solved using the MINLP solvers DICOPT and SBB in GAMS [28]. The algorithm in DICOPT is based on the outer approximation method combined with the equality relaxation technique. The algorithm in SBB is based on a combination of the standard branch and bound method and some effective NLP solvers. Table 9 compares the results and performances of the proposed method, DICOPT and SBB.

As shown in Table 9, the objective value of the proposed method is 0.56% less than DICOPT. The time of the proposed method is only 2.3% of DICOPT. Compared with the existing work [18], which also solves a modified IEEE 118-bus case with approximately 9798 s, the

Table 8
UC state of iteration 2 in the IEEE-30 case.

Units	Hours (1–24)					
	1–4	5–8	9–12	13–16	17–20	21–24
G1	1 1 1 1	1 1 1 1	1 1 1 1	1 1 1 1	1 1 1 1	1 1 1 1
G2	0 0 0 0	0 0 0 0	0 0 0 0	0 0 1 1	1 1 0 0	0 0 0 0
G3	0 0 0 0	0 0 1 1	1 1 1 1	1 1 1 1	1 1 1 1	1 1 1 1
G4	1 1 1 1	1 1 1 1	1 1 1 1	1 1 1 1	1 1 1 1	1 1 1 1
G5	1 1 0 0	0 0 0 0	0 0 1 1	1 1 1 1	1 1 1 1	1 1 0 0
G6	0 0 0 0	0 0 0 0	0 0 0 0	0 0 0 0	0 0 0 0	0 0 0 0

Table 9
Results of the proposed method, DICOPT and SBB.

	CPU time (s)	Objective (MBtu)	Transmission losses (MWh)
Proposed method	321	711,840	2572
DICOPT	14,130	715,831	2401
SBB	No feasible solution found after 12 h		

Table 10
Results of the proposed method, DICOPT and SBB in tighter case.

	CPU time (s)	Objective (MBtu)	Transmission losses (MWh)
Proposed Method	569	712,452	2578
DICOPT	16,197	715,750	2401
SBB	No feasible solution found after 12 h		

CPU time of the proposed method is only 3.3% of the method in Ref. [18]. These data indicate that the main advantage of the proposed method is that it combines high computational efficiency with satisfactory accuracy.

It is worth clarifying that the concept *accuracy* is complicated here because the AC-NCUC problem is a non-convex MINLP problem. None of the proposed method, DICOPT, SBB and the existing AC-NCUC methods ensure a global optimum for this type of problem; hence, we cannot use a direct and rigorous way, *i.e.*, obtaining the global optimum to evaluate the accuracy of our solution for large cases. In addition, it is hard to evaluate the solution accuracy in an analytical way. Although the goal of the proposed method is not to ensure the global optimum, we can still gain some understanding of its solution quality by comparing it with the available powerful MINLP solvers. Because DICOPT provides its optimal solution before the computation approaches its time limit (12 h), it is credible that the solution quality is not influenced by the time limit. The solution obtained by DICOPT, which is a relatively mature and highly popular MINLP solver of all MINLP solvers in GAMS, probably has satisfactory accuracy that is not very far away from the global optimum. Therefore, although it is not a rigorous way, the solution comparison between DICOPT and the proposed method is helpful to understand the solution quality of our method.

A more stressed voltage feasibility situation is also used to further validate the robustness of the proposed method by tightening the bus voltage limit from 1.06/0.94 to 1.05/0.95. Four iterations are required for the proposed method to solve this tighter case. Table 10 compares the proposed method, DICOPT and SBB for this tighter case. With the tighter voltage limit, the proposed method still exhibits a satisfactory solution and efficiency because its objective value is 0.46% less than DICOPT and the CPU time is only 3.5% of DICOPT.

5. Conclusion

In this paper, a decomposition method is proposed for the AC-NCUC problem. By solving the MISOCP model of the master problem, the active power and reactive power are co-optimised based on the conic approximations of the AC power flow equations to provide a better UC solution than the solution from the DC power flow-based model. This better UC solution can be obtained because the MISOCP model respects part of the nonlinearity of the AC power flow equations. Next, the subproblems determine the AC power flow feasibility for the UC solution. V-Q constraints that pinpoint voltage violations in a "one-on-one" manner are introduced into the master problem to reschedule the UC and eliminate the AC infeasibility. A salient feature is that they reflect the quantitative effect of the reactive power of most effective units on correcting the bus voltage violations. Case studies show that with satisfactory solutions obtained, the proposed method can significantly enhance the computational efficiency in solving the AC-NCUC problem. Our future work is directed at investigating the possibility of a global optima convergence.

Acknowledgements

This work is supported by the National Natural Science Foundation of China (No. 51325702, No. 51407100), the China Postdoctoral Science Foundation (No. 2014M560969) and the scholarship under the State Scholarship Fund of China Scholarship Council (File No. 201406210197).

Appendix

The $\mathbf{Q}-\mathbf{V}$ equation in the fast decoupled load flow [29] is

$$-\mathbf{B}''\Delta\mathbf{V} = \Delta\mathbf{Q}/\mathbf{V}, \tag{29}$$

where $\Delta\mathbf{V}$ and $\Delta\mathbf{Q}$ are only used for PQ-type buses (load buses). Ignore the voltage magnitude in $\Delta\mathbf{Q}/V$ and extend (29) to include PV-type buses (generator buses). Then,

$$-\begin{bmatrix}\mathbf{L_{DD}} & \mathbf{L_{DG}}\\ \mathbf{L_{GD}} & \mathbf{L_{GG}}\end{bmatrix}\begin{bmatrix}\Delta\mathbf{V_D}\\ \Delta\mathbf{V_G}\end{bmatrix} = \begin{bmatrix}\Delta\mathbf{Q_D}\\ \Delta\mathbf{Q_G}\end{bmatrix}, \tag{30}$$

where $\mathbf{L_{DD}}$ is $\mathbf{B}''$ in (29), $\mathbf{L_{DG}}$ and $\mathbf{L_{GD}}$ are the imaginary part of the mutual admittance between PQ-type buses and PV-type buses, and $\mathbf{L_{GG}}$ is the imaginary part of the self-admittance of PV-type buses. In other words, $\mathbf{L_{DD}}$,$\mathbf{L_{DG}}$,$\mathbf{L_{GD}}$ and $\mathbf{L_{GG}}$ are the corresponding imaginary part of the admittance matrix. Thereafter, consider

$$\begin{bmatrix}\mathbf{R_{DD}} & \mathbf{R_{DG}}\\ \mathbf{R_{GD}} & \mathbf{R_{GG}}\end{bmatrix} = -\begin{bmatrix}\mathbf{L_{DD}} & \mathbf{L_{DG}}\\ \mathbf{L_{GD}} & \mathbf{L_{GG}}\end{bmatrix}^{-1}. \tag{31}$$

Because there are no generators at PQ-type buses, the reactive power injection at these buses is constant (*i.e.*, $\Delta\mathbf{Q_D} = 0$). With (31) and $\Delta\mathbf{Q_D} = 0$, we can obtain

$$\Delta\mathbf{V_D} = \mathbf{R_{DG}}\Delta\mathbf{Q_G} \tag{32}$$

$$\Delta\mathbf{V_G} = \mathbf{R_{GG}}\Delta\mathbf{Q_G}. \tag{33}$$

Hence, $\mathbf{R_{DG}}$ contains the sensitivity of the voltage magnitude at load buses to a change in reactive power injection at generator buses, and $\mathbf{R_{GG}}$ contains the sensitivity of the voltage magnitude at generator buses to a change in reactive power injection at generator buses. Therefore, $\pi_{i,k}$ that is used in Section 3.4 is the corresponding element in these two matrices. Specifically, assume that unit k is located at bus j. If bus i is a load bus, $\pi_{i,k}$ is the element at the (i,j) position of $\mathbf{R_{DG}}$. If bus i is a generator bus, $\pi_{i,k}$ is the element at the (i,j) position of $\mathbf{R_{GG}}$.

References

[1] Dvorkin Y, Pandzic H, Ortega-Vazquez MA, Kirschen DS. A hybrid stochastic/interval approach to transmission-constrained unit commitment. IEEE Trans Power Syst 2014:1–11.
[2] Lei W. An improved decomposition framework for accelerating LSF and BD based methods for network-constrained UC problems. IEEE Trans Power App Syst 2013;28:3977–86.
[3] Ayoub AK, Patton AD. Optimal thermal generating unit commitment. IEEE Trans Power App Syst 1971;PAS-90(4):1752–6.
[4] Chattopadhyay D, Momoh J. A multiobjective operations planning model with unit commitment and transmission constraints. IEEE Trans Power Syst 1999;14(3):1078–84.

[5] Yuan L, McCalley JD and Ryan S. Risk-based Unit commitment in Proceedings of the 2007 IEEE Power & Energy Society General Meeting.
[6] Qianfan W, Jianhui W, Yongpei G. Stochastic unit commitment with uncertain de-mand response. IEEE Trans Power Syst 2013;28(1):562–3.
[7] Ji B, Yuan X, Chen Z, Tian H. Improved gravitational search algorithm for unit commitment considering uncertainty of wind power. Energy 2014;67:52–62.
[8] Madzharov D, Delarue E, D'Haeseleer W. Integrating electric vehicles as flexible load in unit commitment modeling. Energy 2014;65:285–94.
[9] Crespo JM, Usaola J, Fernandez J. Security-constrained optimal generation scheduling in large-scale power systems. IEEE Trans Power Syst 2006;21(1):321–32.
[10] Bhattacharya K, Zhong J. Reactive power as an ancillary service. IEEE Trans Power Syst 2001;16:294–300.
[11] Recent ISO software enhancements and future software and modeling plans. FERC; 2011 [Online]. available, http://www.ferc.gov/industries/electric/indusact/rto/rto-iso-soft-2011.pdf [Dec 5, 2014].
[12] Kim JS, Edgar TF. Optimal scheduling of combined heat and power plants using mixed-integer nonlinear programming. Energy 2014;77:675–90.
[13] Murillo-Sanchez Carlos, Thomas Robert J. Thermal unit commitment including optimal AC power flow constraints. Proc. The 31th Hawaii international conf. system sciences, vol. 3; 1998. IEEE.
[14] Yong F, Shahidehpour M, Zuyi L. Security-constrained unit commitment with ac constraints*. IEEE Trans Power Syst 2005;20(3):1538–50.
[15] Sifuentes WS, Vargas A. Hydrothermal scheduling using benders decomposition: accelerating techniques. IEEE Trans. Power Syst 2007;22(3):1351–9.
[16] Lavaei J, Low SH. Zero duality gap in optimal power flow problem. IEEE Trans Power Syst 2012;27(1):92–107.
[17] Bai X, Wei H, Fujisawa K, Wang Y. Semidefinite programming for optimal power flow problems. Int J Electr Power Energ Syst 2008;30:383–92.
[18] Bai X, Wei H. Semi-definite programming-based method for security-constrained unit commitment with operational and optimal power flow constraints. IET Gen Trans Distrib 2009;3(2):182–97.
[19] Farivar M, Low SH. Branch flow model: relaxations and convexification-part I. IEEE Trans Power Syst 2013;28(3):2554–64.
[20] Sojoudi S and Lavaei J. Physics of power networks makes hard optimization problems easy to solve, in Proceedings of the 2011 IEEE Power & Energy Society General Meeting.
[21] Jabr RA. Radial distribution load flow using conic programming. IEEE Trans Power Syst 2006;21:1458–9.
[22] Taylor JA, Hover FS. Conic ac transmission system planning. IEEE Trans. Power Syst 2013;28(2):952–9.
[23] Yuan X, Tian H, Zhang S, Ji B, Hou Y. Second-order cone programming for solving unit commitment strategy of thermal generators. Energy Convers Manag 2013;76:20–5.
[24] Carrion M, Arroyo JM. A computationally efficient mixed-integer linear formulation for the thermal unit commitment problem. IEEE Trans. Power Syst 2006;21(3):1371–8.
[25] Grainger John J, Stevenson William D. Power system analysis, vol. 621. New York: McGraw-Hill; 1994.
[26] Gurobi. [Online]. Available: http://www.gurobi.com/. [Jan 12, 2015].
[27] Wächter A, Biegler LT. On the implementation of a primal-dual interior point filter line search algorithm for large-scale nonlinear programming. Math Program 2006;106(1):25–57.
[28] GAMS. [Online]. Available: http://www.gams.com/default.html [Jan 12, 2015].
[29] Stott B, Alsac O. Fast decoupled load flow. IEEE Trans Power App Syst 1974;PAS-93(3):859–69.
[30] Power system test case archive. Univ. Washington, lect. Eng Dept. E. 2007 [Online]. Available, https://www.ee.washington.edu/research/pstca/index.html [Feb 5, 2015].